Reply to comments from Referee #1

First of all, thank you for your valuable comments and suggestions. Following your comments, we attempt to clarify and improve the manuscript by eliminating, modifying, and adding several parts from/into the original text. The added or modified parts are painted in a blue color in the revised manuscript.

General Comment

In this study, the author attempted to sequentially incorporate several potential HONO sources and processes into the CMAQ modeling framework. And the simulation performances of the modified CMAQ models were then evaluated by comparing the modeled HONO mixing ratios with the HONO mixing ratios observed at the Olympic Park station in Seoul, South Korea. The simulation results have been improved than the Original CMAQ model. However, there are several issues in the article.

Specific Comments

Comment 1 In Lines 179-180, the average values of simulation results in Table S2 are not sufficient to confirm the good prediction of the model, and the comparisons of time series of observation and modeled outputs are needed.

Reply: Considering your comments, we added Fig. S1 and revised Table S2 into the supplementary material. Fig. S1 shows the temporal variations of modeled and observed relative humidity (RH), temperature (T), pressure (P), wind speed (WS), and wind direction (WD) during the target periods. Please, refer to Fig. S1 and Table S2. The purpose of original Table S2 was that our meteorological model simulations produced reasonable quality of meteorological fields.

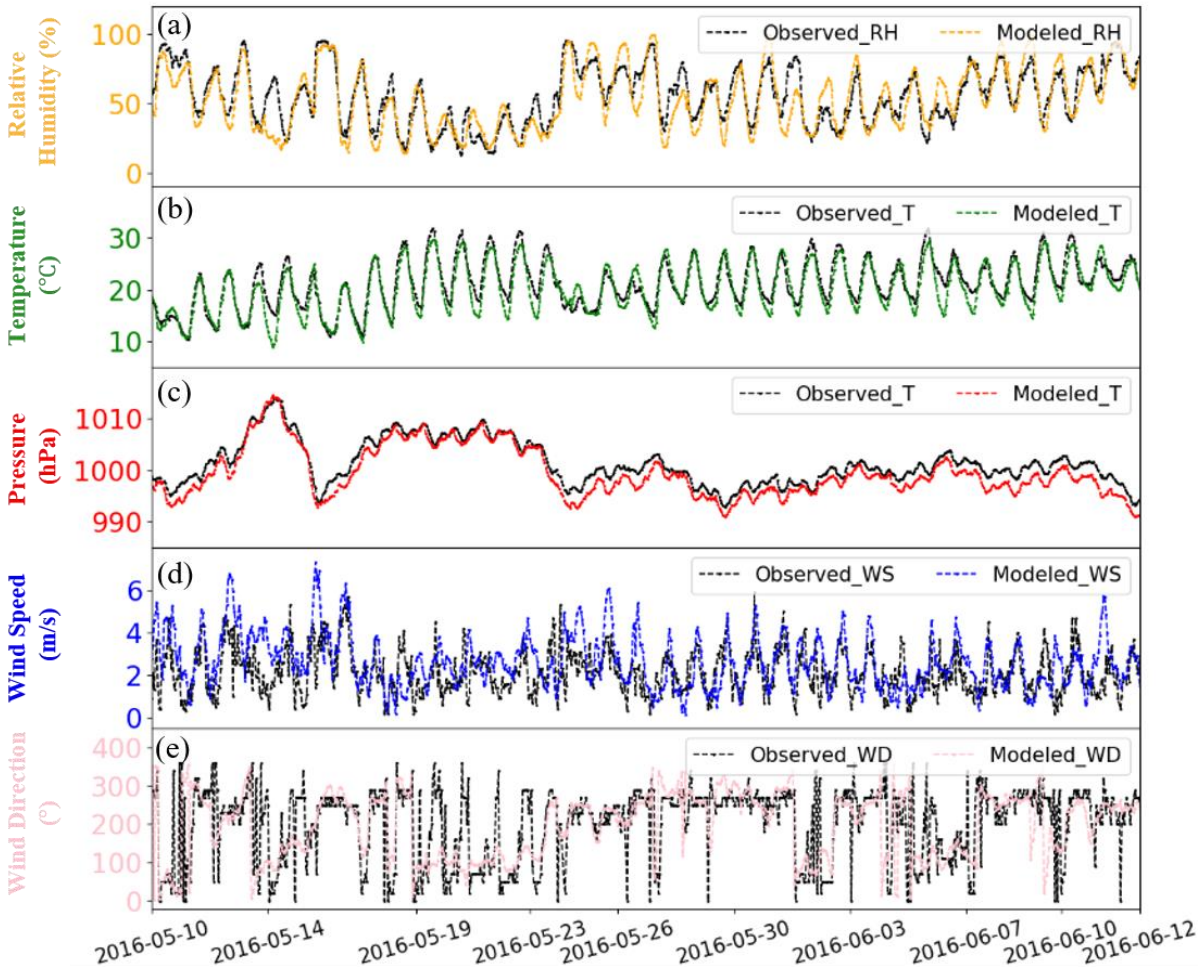

Fig. S1. Temporal variations of (a) relative humidity (RH); (b) temperature (T); (c) pressure; (d) Wind speed (WS) at 10m above the surface; and (e) wind direction (WD) at 10m above the surface during period of the KORUS-AQ campaign.

Table S2. Statistical analysis of modeled and observed meteorological parameters at the Olympic Park station during the period of the KORUS-AQ campaign.

Parameter	Observed mean	Modeled mean	R	RMSE	MB	IOA
RH (%)	55.81	53.33	0.85	11.95	-2.48	0.92
T (℃)	21.27	20.28	0.93	1.96	-0.99	0.96
Pressure (hPa)	1001.38	999.62	0.98	2.01	-1.77	0.95
WS (m s^{-1})	2.14	2.65	0.47	1.30	0.51	0.66
WD (°)	202.71	196.01	0.53	88.87	-6.70	0.75

Comment 2 In Table 1, the emission factor of gasoline and diesel vehicles are 0.8% and 2.3% in all studies area. However, there are significant differences in traffic volumes and vehicle types in different areas.

Reply: The traffic emissions used in this study were from the anthropogenic emissions inventory of KORUSv5.0. The KORUSv5.0 was developed based on detailed considerations of vehicle fuel-types and traffic volumes across our domain (East Asia) (Please, refer to Woo et al., 2012; Woo et al., 2020).

Comment 3 In lines 205-207, is the equation for the relationship between J_{NPHE} and J_{NO2} also in this reference (Stockwell et al., 1990)? And how J_{HONO} is calculated?

Reply: The relationship between J_{NPHE} and J_{NO2} was first proposed by Bejan et al. (2006). Since then, it has been utilized in many modeling mechanisms, including SAPRC07TC (Carter et al., 2010). Regarding this, please refer to lines 207-208 in our revised manuscript.
The J values for HONO and other chemical species were calculated in CMAQ modeling via PHOT subroutine, using quantum yields and cross-section data. In our CMAQ model simulations, they were calculated based on a look-up table involving J_values at different latitudes, altitudes, and solar zenith angles. After the initial J values were calculated under the clear-sky conditions, such values were corrected with cloud coverage data (Byun and Ching, 1999).

Comment 4 In Table 3, how were HONO emission rates of traffic calculated?

Reply: The HONO emissions were determined based on the emission ratios of HONO to NO_x from gasoline and diesel vehicle exhausts. These ratios were discussed in lines 233-235 in our revised manuscript.

Comment 5 In lines 276-277, why are the uptake coefficients of NO_2 at nighttime and daytime are 8.0×10^{-6} and 1.3×10^{-4}, respectively? Also how is the 900 for this factor taken into account? The same issue in lines 292-293.

Reply: We adopted the uptake coefficients of NO_2 on aerosol and ground surfaces from the studies of Czader et al. (2012) and VandenBoer et al. (2013). Also, the factor was selected to be 900 $W\cdot m^{-2}$ based on a sensitivity test (Czader et al., 2012). We clarified this point in our revised manuscript (Please, refer to lines 281 – 282, 296 – 297, and Table R1).

Table R1. Statistical analysis with different parameterization of γ_{NO_2} for modeled and observed HONO mixing ratios at the Olympic Park stations, Seoul, Korea.

EXP	Parameterizations of γ_{NO_2}		References	Observed mean	Modeled mean	IOA	MB	RMSE
SEN_A	$\gamma_{a,NO_2} = 2.0 \times 10^{-5} \times (\frac{\text{light intensity}}{400})$	(daytime)	Kleffmann et al. (1998) Vogel et al. (2003) Zhang et al. (2023) Marion et al. (2021)	1.35	1.44	0.654	0.09	1.28
	$\gamma_{a,NO_2} = 1.0 \times 10^{-6}$	(nighttime)						
	$\gamma_{g,NO_2} = 1.3 \times 10^{-6} + 4.8 \times 10^{-8} \times [SWR]$	(daytime)						
	$\gamma_{g,NO_2} = 6.5 \times 10^{-7}$	(nighttime)						
SEN_B	$\gamma_{a,NO_2} = 1.3 \times 10^{-4} \times (\frac{\text{light intensity}}{400})$	(daytime)	Xue et al. (2021) Mong et al. (2009) Yu et al. (2021)	1.35	1.18	0.713	-0.17	1.11
	$\gamma_{a,NO_2} = 2.0 \times 10^{-6}$	(nighttime)						
	$\gamma_{g,NO_2} = 5.8 \times 10^{-6} \times (\frac{\text{light intensity}}{400})$	(daytime)						
	$\gamma_{g,NO_2} = 3.1 \times 10^{-7}$	(nighttime)						
SEN_C	$\gamma_{a,NO_2} = 4.0 \times 10^{-5} \times (\frac{\text{light intensity}}{400})$	(daytime)	Stemmler et al. (2007) Liu et al. (2019) Yu et al. (2021)	1.35	1.13	0.729	-0.22	1.06
	$\gamma_{a,NO_2} = 8.0 \times 10^{-6}$	(nighttime)						
	$\gamma_{g,NO_2} = 5.8 \times 10^{-6} \times (\frac{\text{light intensity}}{400})$	(daytime)						
	$\gamma_{g,NO_2} = 3.1 \times 10^{-7}$	(nighttime)						
SEN_D	$\gamma_{a,NO_2} = 2.0 \times 10^{-5} \times (\frac{\text{light intensity}}{400})$	(daytime)	Kleffmann et al. (1998) Vogel et al. (2003) Yu et al. (2021)	1.34	1.62	0.733	0.27	1.02
	$\gamma_{a,NO_2} = 1.0 \times 10^{-6}$	(nighttime)						
	$\gamma_{g,NO_2} = 5.8 \times 10^{-6} \times (\frac{\text{light intensity}}{400})$	(daytime)						
	$\gamma_{g,NO_2} = 3.1 \times 10^{-7}$	(nighttime)						
SEN_E	$\gamma_{a,NO_2} = 4.0 \times 10^{-5} \times (\frac{\text{light intensity}}{900})$	(daytime)	Stemmler et al. (2007) Liu et al. (2019) Yu et al. (2021) Vandenboer et al. (2013)	1.35	1.05	0.742	-0.30	1.06
	$\gamma_{a,NO_2} = 8.0 \times 10^{-6}$	(nighttime)						
	$\gamma_{g,NO_2} = 5.8 \times 10^{-6} \times (\frac{\text{light intensity}}{900})$	(daytime)						
	$\gamma_{g,NO_2} = 3.1 \times 10^{-7}$	(nighttime)						
SEN_F	$\gamma_{a,NO_2} = 1.3 \times 10^{-4} \times (\frac{\text{light intensity}}{900})$	(daytime)	This study	1.35	1.18	0.764	-0.17	1.12
	$\gamma_{a,NO_2} = 8.0 \times 10^{-6}$	(nighttime)						
	$\gamma_{g,NO_2} = 5.8 \times 10^{-6} \times (\frac{\text{light intensity}}{900})$	(daytime)						
	$\gamma_{g,NO_2} = 5.0 \times 10^{-7}$	(nighttime)						

Comment 6 In Line 412, is there much improvement in model results if NO_2 daytime sources are enhanced?

Reply: The consideration of photo-induced NO_2-to-HONO conversion improved the mean bias from -0.79 to -0.28 ppb (please, refer to Fig. 3 or Table 4). However, there is still room for further improvements, with respect to direct HONO emissions and vertical parameterizations of NO_2 (Gilgorovski et al., 2016; Guo et al., 2020; Tang et al., 2024).

Comment 7 In Line 447, "Its contribution increases to 4.2% during the daytime", which sources is this contribution?

Reply: The "Its contribution" meant the contribution from the HET_A during the daytime. However, this sentence was removed in our revised manuscript, because we thought it is a little bit out of context.

Reference cited in this response:

Woo, J.-H., Choi, K.-C., Kim, H.K., Baek, B.H., Jang, M., Eum, J.-H., Song, C.H., Ma, Y.-I., Sunwoo, Y., Chang, L.-S., 2012. Development of an anthropogenic emissions processing system for Asia using SMOKE. Atmospheric environment 58, 5-13.

Woo, J.-H., Kim, Y., Kim, H.-K., Choi, K.-C., Eum, J.-H., Lee, J.-B., Lim, J.-H., Kim, J., Seong, M., 2020. Development of the CREATE Inventory in Support of Integrated Climate and Air Quality Modeling for Asia. Sustainability 12, 7930.

Bejan, I., Abd El Aal, Y., Barnes, I., Benter, T., Bohn, B., Wiesen, P., & Kleffmann, J. (2006). The photolysis of ortho-nitrophenols: a new gas phase source of HONO. *Physical Chemistry Chemical Physics*, *8*(17), 2028-2035.

Carter, W.P.L. (2010). "Development of the SAPRC-07 chemical mechanism and updated ozone reactivity scales." *International Journal of Chemical Kinetics*, 42(4), 273-290.

Byun, D. W., & Ching, J. K. S. (Eds.). (1999). *Science algorithms of the EPA Models-3 community multiscale air quality (CMAQ) modeling system* (p. 727). Washington, DC: US Environmental Protection Agency, Office of Research and Development.

Czader, B. H., Rappenglück, B., Percell, P., Byun, D. W., Ngan, F., & Kim, S. (2012). Modeling nitrous acid and its impact on ozone and hydroxyl radical during the Texas Air Quality Study 2006. *Atmospheric Chemistry and Physics*, *12*(15), 6939-6951.

Kleffmann, J., Becker, K. H., & Wiesen, P. (1998). Heterogeneous NO2 conversion processes on acid surfaces: possible atmospheric implications. Atmospheric Environment, 32(16), 2721-2729.

Vogel, B., Vogel, H., Kleffmann, J., & Kurtenbach, R. (2003). Measured and simulated vertical profiles of nitrous acid—Part II. Model simulations and indications for a photolytic source. Atmospheric environment, 37(21), 2957-2966.

Zhang, X., Tong, S., Jia, C. *et al.* Elucidating HONO formation mechanism and its essential contribution to OH during haze events. *npj Clim Atmos Sci* **6**, 55 (2023).

Marion, A., Morin, J., Gandolfo, A., Ormeño, E., D'Anna, B., & Wortham, H. (2021). Nitrous acid formation on Zea mays leaves by heterogeneous reaction of nitrogen dioxide in the laboratory. Environmental Research, 193, 110543.

Xue, C., Ye, C., Kleffmann, J., Zhang, C., Catoire, V., Bao, F., Mellouki, A., Xue, L., Chen, J., Lu, K., Zhao, Y., Liu, H., Guo, Z., and Mu, Y.: Atmospheric measurements at Mt. Tai – Part I: HONO formation and its role in the oxidizing capacity of the upper boundary layer, Atmos. Chem. Phys., 22, 3149–3167, 2022.

Monge, M. E., D'Anna, B., Mazri, L., Giroir-Fendler, A., Ammann, M., Donaldson, D. J., & George, C. (2010). Light changes the atmospheric reactivity of soot. Proceedings of the National Academy of Sciences, 107(15), 6605-6609.

Yu, C., Wang, Z., Ma, Q., Xue, L., George, C., & Wang, T. (2021). Measurement of heterogeneous uptake of NO2 on inorganic particles, sea water and urban grime. Journal of Environmental Sciences, 106, 124-135.

Stemmler, K.; Ndour, M.; Elshorbany, Y.; Kleffmann, J.; D'Anna, B.; George, C.; Bohn, B.; Ammann, M., Light 146 induced conversion of nitrogen dioxide into nitrous acid on submicron humic acid aerosol. Atmos. Chem. Phys. 2007, 7,147 (16), 4237-4248

Liu, Y., Lu, K., Li, X., Dong, H., Tan, Z., Wang, H., Zou, Q., Wu, Y., Zeng, L., Hu, M., Min, K.-E., Kecorius, S., Wiedensohler, A., and Zhang, Y.: A Comprehensive Model Test of the HONO Sources Constrained to Field Measurements at Rural North China Plain, Environ. Sci. Technol., 53, 3517–3525, 2019.

VandenBoer, T. C., et al. (2013), Understanding the role of the ground surface in HONO vertical structure: Highresolution vertical profiles during NACHTT-11, J. Geophys. Res. Atmos., 118, 10,155–10,171

Gligorovski, S. (2016). Nitrous acid (HONO): An emerging indoor pollutant. *Journal of Photochemistry and Photobiology A: Chemistry*, *314*, 1-5.

Guo, Y., Zhang, J., An, J., Qu, Y., Liu, X., Sun, Y., & Chen, Y. (2020). Effect of vertical parameterization of a missing daytime source of HONO on concentrations of HONO, O3 and secondary organic aerosols in eastern China. *Atmospheric Environment*, *226*, 117208.

Tang, M.-X.; He, L.-Y.; Xia, S.-Y.; Jiang, Z.; He, D.-Y.; Guo, S.; Hu, R.-Z.; Zeng, H.; Huang, X.-F. Coarse particles compensate for missing daytime sources of nitrous acid and enhance atmospheric oxidation capacity in a coastal atmosphere. *Science of The Total Environment* 2024, *915*,

Reply to comments from Referee #2

First of all, thank you for your valuable comments and suggestions. Following your comments, we attempt to clarify and improve the manuscript by eliminating, modifying, and adding several parts from/into the original text. The added or modified parts are painted in a blue color in the revised manuscript.

General Comment

The manuscript titled "Investigation of the atmospheric nitrous acid (HONO) process in South Korea" by Kiyeon Kim et al. examined the contribution of various sources to HONO formation through detailed model simulations. Additionally, the study also investigated the impact of HONO processes on atmospheric species such as OH, HO2, HCHO, and O3 etc. Overall, the manuscript is well-written and organized; however, there are several questions that need to be addressed before it can be published.

Specific Comments

Comment 1. Line 345: The author suggested that the WRF model exhibits a pronounced inclination to generate higher wind speeds compared to actual measurements, which may result in an underestimation of air pollutant concentrations. If this assertion holds true, it is reasonable to assume that such underestimations would also occur during other periods. Could you provide further clarification or explanations regarding the underestimation observed during stagnant periods?

Reply: As reviewer pointed out, the overestimations of wind speeds influence the mixing ratios of HONO throughout the entire period. To clarify this explanation, we analyzed wind speeds for the stagnant period. During the entire KORUS-AQ period, average simulated wind speed is 2.65 m/s, 23.8% faster than average observed wind speed of 2.14 m/s. However, average simulated wind speed during the stagnant period is 2.59 m/s, 36.3% faster than average observed wind speed of 1.90 m/s. Based on this, we believe that the simulated wind speeds under the stagnant condition influence the mixing ratios of HONO much more than those during other periods. We added this point in our revised manuscript (Please, refer to lines 348 – 351).

Comment 2. In EXP 2, the authors assess the impact of biomass burning on HONO emissions. It is acknowledged that there is no significant biomass burning occurring during this period, thus the direct contribution of biomass burning can be considered negligible. However, has the author taken into account the potential secondary formation from these sources? For instance, recent studies have reported an increased formation of HONO in the presence of nitrate and

organics (e.g., photosensitizer) under irradiation (Jiang et al., 2023; Wang et al., 2021), which could be emitted from biomass burning. Furthermore, it has also been documented that HONO generation can occur through reactions between nitrate and Fe(II) promoted by photolysis of Iron-organic complexes (Gen et al., 2021). Considering that all these components may originate from biomass burning, it would be worthwhile to investigate the influence of these secondary reactions on HONO formation.

Reply: Thank you for your comment on potential HONO formation. Many lab-scale experiments and field observations have been carried out to find the missing HONO formation pathways, including those suggested by reviewer (Jiang et al., 2023; Gen et al., 2021; Wang et al., 2021). However, in order to simulate these processes in the 3D-CTM framework, the emission fluxes of humic acid, vanillic acid, iron-organic compounds, etc., are required. Our current emissions do not include these details. Thus, the HONO formation pathways mentioned by reviewer could not be considered in our CTM simulations.

Nevertheless, because the discrepancy between the simulated and observed HONO mixing ratios can be resulted from these missing reactions, we mentioned them in our revised manuscript (Please, refer to lines 368-371 and 428-430). Also, the renoxification of HNO_3 and nitrate considered in our study may be somehow similar to the reaction mentioned by reviewer. On the other hand, large-scale biomass-burning events did not take place in South Korea during our simulation period, according to the FINN emission. The emissions of nitrate and organic carbon from the biomass burning events may also be almost negligible. Figure R1 presents spatial distributions of these emissions.

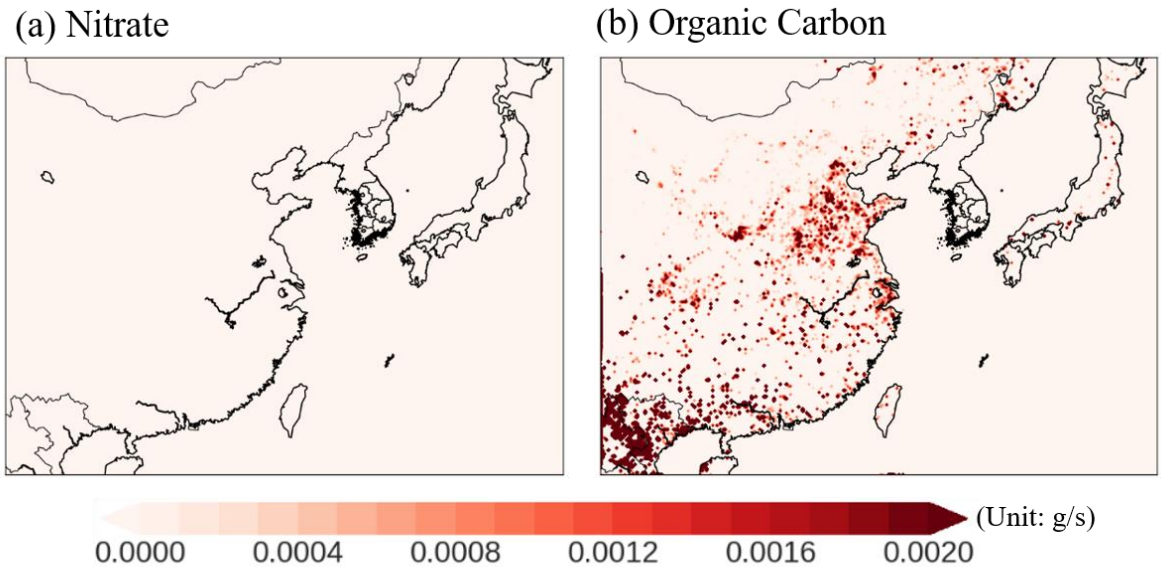

Fig. R1. Spatial distributions of (a) nitrate and (b) organic carbon emission rates in the FINNv1.5 inventory over the East Asia during the period of the KORUS-AQ campaign.

Comment 3. Line 376-377: Are there any specific reasons why the soil emissions of HONO are not considered significant in South Korea?

Reply: As reported in other studies (e.g., An et al., 2023; Kim et al., 2008), the emissions of soil NO_x estimated from the MEGAN model simulations were significantly low in South Korea. These low NO_x emissions from soils may be linked to several factors: (i) geographical feature mainly covered by forest and mountain areas; (ii) use of low nitrogen fertilizers; and (iii) low availability of nitrogen in the soils due to acidic deposition from the air. In addition to these factors, the soil water content (SWC), which is a main factor used for the estimation of soil HONO emissions, is relatively high in South Korea (refer to Fig. R2), which leads to high soil pH. We added these discussions in our revised manuscript (Please, refer to lines 384 - 389).

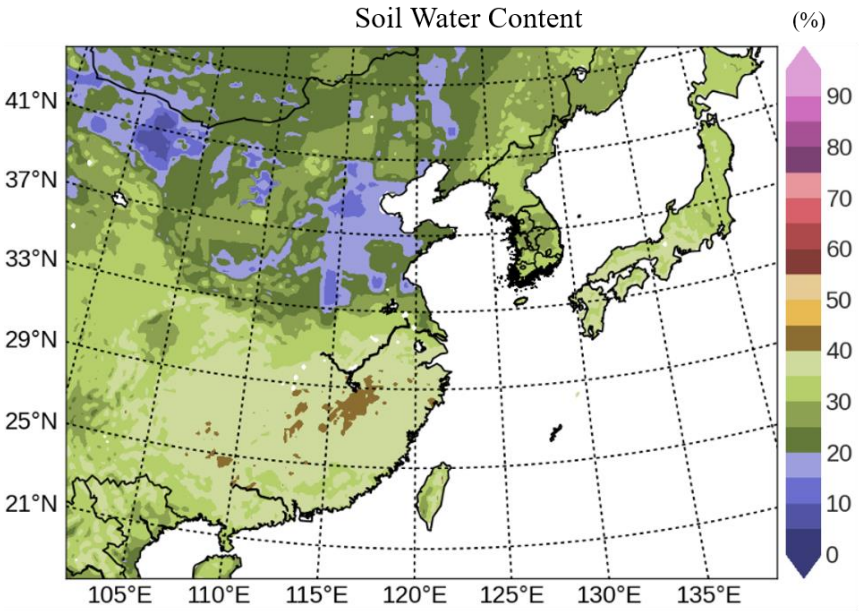

Fig. R2. Spatial distributions of Soil Water Content (SWC) over the East Asia during the period of the KORUS-AQ campaign

Comment 4. Line 378-380: Have the authors conducted any sensitivity tests, such as investigating the impact of an increased uptake coefficient of NO2 on heterogeneous NO2 reactions and subsequent HONO formation?

Reply: Yes, we have conducted sensitivity tests. The results of the sensitivity tests are summarized in Table R1. Based on these sensitivity tests, we actually selected the uptake coefficient of NO_2 in our study.

Table R1. Statistical analysis with different parameterization of γ_{NO_2} for modeled and observed HONO mixing ratios at the Olympic Park stations, Seoul, Korea.

EXP	Parameterizations of γ_{NO_2}		References	Observed mean	Modeled mean	IOA	MB	RMSE
SEN_A	$\gamma_{a,NO_2} = 2.0 \times 10^{-5} \times (\frac{\text{light intensity}}{400})$	(daytime)	Kleffmann et al. (1998) Vogel et al. (2003) Zhang et al. (2023) Marion et al. (2021)	1.35	1.44	0.654	0.09	1.28
	$\gamma_{a,NO_2} = 1.0 \times 10^{-6}$	(nighttime)						
	$\gamma_{g,NO_2} = 1.3 \times 10^{-6} + 4.8 \times 10^{-8} \times [SWR]$	(daytime)						
	$\gamma_{g,NO_2} = 6.5 \times 10^{-7}$	(nighttime)						
SEN_B	$\gamma_{a,NO_2} = 1.3 \times 10^{-4} \times (\frac{\text{light intensity}}{400})$	(daytime)	Xue et al. (2021) Mong et al. (2009) Yu et al. (2021)	1.35	1.18	0.713	-0.17	1.11
	$\gamma_{a,NO_2} = 2.0 \times 10^{-6}$	(nighttime)						
	$\gamma_{g,NO_2} = 5.8 \times 10^{-6} \times (\frac{\text{light intensity}}{400})$	(daytime)						
	$\gamma_{g,NO_2} = 3.1 \times 10^{-7}$	(nighttime)						
SEN_C	$\gamma_{a,NO_2} = 4.0 \times 10^{-5} \times (\frac{\text{light intensity}}{400})$	(daytime)	Stemmler et al. (2007) Liu et al. (2019) Yu et al. (2021)	1.35	1.13	0.729	-0.22	1.06
	$\gamma_{a,NO_2} = 8.0 \times 10^{-6}$	(nighttime)						
	$\gamma_{g,NO_2} = 5.8 \times 10^{-6} \times (\frac{\text{light intensity}}{400})$	(daytime)						
	$\gamma_{g,NO_2} = 3.1 \times 10^{-7}$	(nighttime)						
SEN_D	$\gamma_{a,NO_2} = 2.0 \times 10^{-5} \times (\frac{\text{light intensity}}{400})$	(daytime)	Kleffmann et al. (1998) Vogel et al. (2003) Yu et al. (2021)	1.34	1.62	0.733	0.27	1.02
	$\gamma_{a,NO_2} = 1.0 \times 10^{-6}$	(nighttime)						
	$\gamma_{g,NO_2} = 5.8 \times 10^{-6} \times (\frac{\text{light intensity}}{400})$	(daytime)						
	$\gamma_{g,NO_2} = 3.1 \times 10^{-7}$	(nighttime)						
SEN_E	$\gamma_{a,NO_2} = 4.0 \times 10^{-5} \times (\frac{\text{light intensity}}{900})$	(daytime)	Stemmler et al. (2007) Liu et al. (2019) Yu et al. (2021) Vandenboer et al. (2013)	1.35	1.05	0.742	-0.30	1.06
	$\gamma_{a,NO_2} = 8.0 \times 10^{-6}$	(nighttime)						
	$\gamma_{g,NO_2} = 5.8 \times 10^{-6} \times (\frac{\text{light intensity}}{900})$	(daytime)						
	$\gamma_{g,NO_2} = 3.1 \times 10^{-7}$	(nighttime)						
SEN_F	$\gamma_{a,NO_2} = 1.3 \times 10^{-4} \times (\frac{\text{light intensity}}{900})$	(daytime)	This study	1.35	1.18	0.764	-0.17	1.12
	$\gamma_{a,NO_2} = 8.0 \times 10^{-6}$	(nighttime)						
	$\gamma_{g,NO_2} = 5.8 \times 10^{-6} \times (\frac{\text{light intensity}}{900})$	(daytime)						
	$\gamma_{g,NO_2} = 5.0 \times 10^{-7}$	(nighttime)						

Comment 5. Figure 3: During the daytime, there is an underestimation of HONO levels even when considering all potential sources. However, an overestimation is observed from 0 am to 6 am when incorporating HET_BD and RENOx. Does this imply the presence of missing sinks for HONO during nighttime? In theory, photolytic renoxification of nitrate should only occur in the presence of irradiation; however, there is an increased concentration of HONO even at night (0 am - 6 am) when including RENOx in the model simulation. Any suggestions on it?

Reply: We believe that the overestimations of HONO mixing ratios for 00:00 am – 06:00 am may be related to the over-predictions of NO_2 mixing ratios. Figure R3 presents diurnal variations of simulated and observed NO_2 mixing ratios. The NO_2 molecules reproduced from reactions 7 and 8 during the daytime (via $RENO_x$) appear to be accumulated within the PBL and are then converted to HONO via the heterogeneous reactions (i.e., via HET_A, HET_BD, and HET_L) during the nighttime.

As reviewer pointed out, the renoxification only takes place in the presence of irradiation. However, in the EXP8 simulation including all the HONO formation processes, HONO appears to be formed further via the heterogeneous reactions of NO_2.

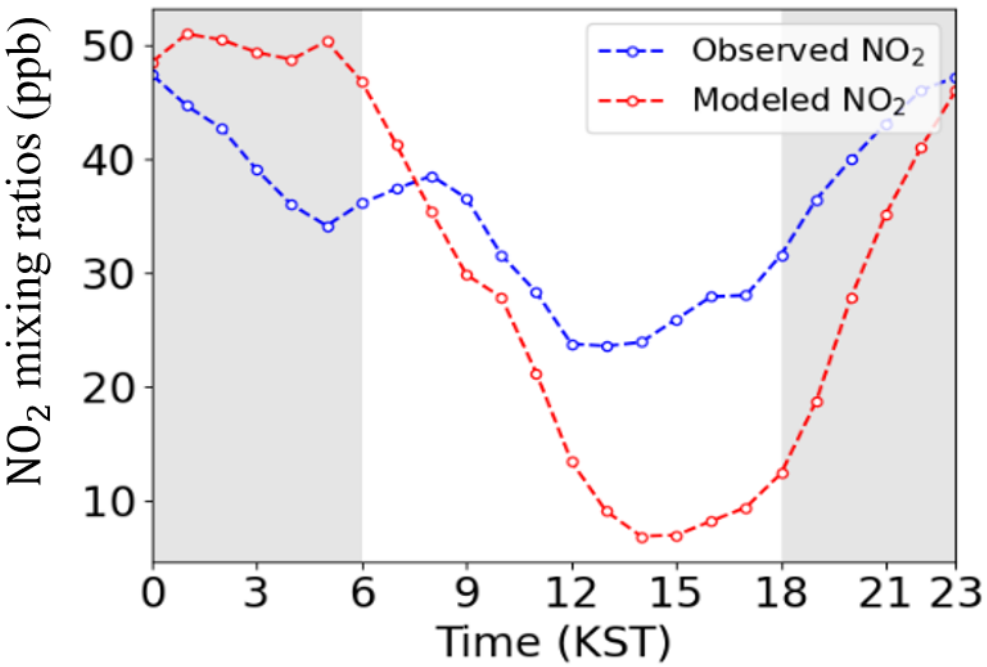

Fig. R3. Diurnal variations of NO_2 mixing ratios from the observation (blue line) and the CMAQ model (red line) during period of the KORUS-AQ campaign

Comment 6. Line 442: It is noteworthy that traffic emissions make a substantial contribution to the overall production of HONO during nighttime. One might assume that traffic would be less prevalent at night compared to daytime. I am curious about how one can differentiate between direct emissions of HONO from traffic and indirect sources, such as NOx emitted from traffic that undergoes further reactions to generate HONO.

Reply: The traffic HONO emissions, the largest contributor to the HONO mixing ratios during the nighttime, were calculated based on constant diurnal anthropogenic NO_x emissions. Due to this reason, the HONO contribution during the nighttime can be somewhat overestimated. We clarified this point in our revised manuscript. (Please, refer to lines 457 - 459).

Secondly, we did not separate the direct HONO emissions from the automobiles from the secondary HONO formation from vehicle-exhausted NO_x in this study. The contribution (TRAF in Fig. 4) to the HONO mixing ratios made by the direct emissions of HONO from the traffic source was simply calculated by subtracting HONO mixing ratios of EXP4 from those of EXP3 simulations.

Comment 7. Line 503-505: The limited contribution of the NO2 + H2O => HONO + NO3 - reaction to HONO formation suggests that its impact on nitrate production is likely negligible, correct? Has the author conducted model simulations to assess its contribution to nitrate?

Reply: Initially, we thought that the heterogeneous reactions of $NO_2 + H_2O \rightarrow NO_3^- + HONO$ increases nitrate concentrations. The heterogeneous reactions of NO_2 on the surfaces of building and leaf actively take place during nighttime, influencing the levels of nitrate by 1.54 $\mu g/m^3$. Regarding this point, please see line 521 in our revised manuscript.

Reference cited in this response:

An, Y., Shim, W., & Jeong, G. (2023). High-Resolution Digital Soil Maps of Forest Soil Nitrogen across South Korea Using Three Machine Learning Algorithms. *Forests*, *14*(6), 1141.

Kim C-H, Park I-S, Kim S-K, Son H-Y, Lee J-J, Lee J-B, Song C-K, Shim J-M (2008) Estimation and mapping of nitrogen uptake by forest in South Korea. Water Air Soil Pollut 187:315–325

Kleffmann, J., Becker, K. H., & Wiesen, P. (1998). Heterogeneous NO2 conversion processes on acid surfaces: possible atmospheric implications. Atmospheric Environment, 32(16), 2721-2729.

Vogel, B., Vogel, H., Kleffmann, J., & Kurtenbach, R. (2003). Measured and simulated vertical profiles of nitrous acid—Part II. Model simulations and indications for a photolytic source. Atmospheric environment, 37(21), 2957-2966.

Zhang, X., Tong, S., Jia, C. *et al.* Elucidating HONO formation mechanism and its essential contribution to OH during haze events. *npj Clim Atmos Sci* **6**, 55 (2023).

Marion, A., Morin, J., Gandolfo, A., Ormeño, E., D'Anna, B., & Wortham, H. (2021). Nitrous acid formation on Zea mays leaves by heterogeneous reaction of nitrogen dioxide in the laboratory. Environmental Research, 193, 110543.

Xue, C., Ye, C., Kleffmann, J., Zhang, C., Catoire, V., Bao, F., Mellouki, A., Xue, L., Chen, J., Lu, K., Zhao, Y., Liu, H., Guo, Z., and Mu, Y.: Atmospheric measurements at Mt. Tai – Part I: HONO formation and its role in the oxidizing capacity of the upper boundary layer, Atmos. Chem. Phys., 22, 3149–3167, 2022.

Monge, M. E., D'Anna, B., Mazri, L., Giroir-Fendler, A., Ammann, M., Donaldson, D. J., & George, C. (2010). Light changes the atmospheric reactivity of soot. Proceedings of the National Academy of Sciences, 107(15), 6605-6609.

Yu, C., Wang, Z., Ma, Q., Xue, L., George, C., & Wang, T. (2021). Measurement of heterogeneous uptake of NO2 on inorganic particles, sea water and urban grime. Journal of Environmental Sciences, 106, 124-135.

Stemmler, K.; Ndour, M.; Elshorbany, Y.; Kleffmann, J.; D'Anna, B.; George, C.; Bohn, B.; Ammann, M., Light
146 induced conversion of nitrogen dioxide into nitrous acid on submicron humic acid aerosol. Atmos. Chem. Phys. 2007, 7,147 (16), 4237-4248

Liu, Y., Lu, K., Li, X., Dong, H., Tan, Z., Wang, H., Zou, Q., Wu, Y., Zeng, L., Hu, M., Min, K.-E., Kecorius, S., Wiedensohler, A., and Zhang, Y.: A Comprehensive Model Test of the HONO Sources Constrained to Field Measurements at Rural North China Plain, Environ. Sci. Technol., 53, 3517–3525, 2019.

VandenBoer, T. C., et al. (2013), Understanding the role of the ground surface in HONO vertical structure: Highresolution vertical profiles during NACHTT-11, J. Geophys. Res. Atmos., 118, 10,155–10,171